



ELSEVIER

Journal of Alloys and Compounds 311 (2000) 60–64

Journal of  
ALLOYS  
AND COMPOUNDS

www.elsevier.com/locate/jallcom

# Effect of rare earth on the microstructures and properties of a low expansion superalloy

R.M. Wang<sup>a,b,\*</sup>, Y.G. Song<sup>a</sup>, Y.F. Han<sup>a</sup><sup>a</sup>Beijing Institute of Aeronautical Materials, P. O. Box 81-4, Beijing 100095, P.R. China<sup>b</sup>Laboratory of Atomic Imaging of Solids, Institute of Metal Research, Chinese Academy of Sciences, Shenyang 110015, P.R. China

## Abstract

A new Fe–Ni–Co–Nb–Ti–Si superalloy containing trace additions of selective rare earths and having with combination of very low thermal expansion coefficient, high resistance to stress accelerated grain boundary oxygen embrittlement and fairly good notch-bar rupture strength has been successfully developed. The resistance to oxidation for long time exposure at high temperatures and the stress rupture life improves significantly with trace yttrium additions. The microstructures of the alloy have been studied by means of analytical electron microscopy and chemical analysis techniques. The results reveal that the rare earth element segregates in the strengthening phase of platelet morphology. Further it helps in transforming  $A_3B$  type  $\epsilon$  phase into  $A_3B$  type H phase. The morphology and crystal structures of the grain boundary phases also change with selective additions of rare earth elements. The platelet precipitates become smaller and denser, and forms within the grains and along the grain boundaries with the additions of rare earth elements. The segregation of the platelet precipitates within the grains is helpful in improving the strength of the alloy. In addition its precipitation along the grain boundaries can improve the resistance to stress accelerated grain boundary oxidation and stress rupture property of the alloy and thereby contributed to its excellent elevated temperature stability. © 2000 Elsevier Science S.A. All rights reserved.

**Keywords:** Fe–Ni–Co–Nb–Ti–Si superalloy; Rare earth element; Micro-mechanism

## 1. Introduction

Incoloy 900 series low expansion superalloys based on the system Fe–Ni–Co–Nb–Ti–Si are attractive for aerospace and land-based gas-turbine engine applications, as they can reduce the clearance necessary between the turbine blade tips and the retainer, simplifying design and substantially improving fuel efficiency [1–3]. The absence of chromium in the alloys makes them very susceptible to oxidation. Of particular concern is the susceptibility of these alloys to stress accelerated grain boundary oxygen embrittlement (SAGBO) [4,5]. The problem can not be generally solved by adjustment of chemical composition and microstructure. One of the possible methods to improve the resistance to SAGBO and the notch rupture strength of the alloys is to add appropriate rare earth elements during fabrication. However, few studies have been reported on this topic. Most of the studies focus on the effect of the rare earth element on steels, aluminium alloys, et al. Lu et al. [6] proposed that the rare earth

elements segregate at the grain boundary, decreasing the martensite grain size in their studies on the low-alloying steel. Zhang et al. [7] found that the segregation of rare earth elements along the grain boundary in phosphorus-containing steel decreased the brittleness from the segregation of phosphorus along the grain boundary. Zhao et al. [8] suggested that rare earth elements affected the separation of the secondary-phases in the study of high-alloying steel. In this paper, the influence of rare earth element on the microstructures and properties of the alloy has been studied by means of transmission electron microscopy, chemical analysis techniques. The micro-mechanism of the property improvement has also been discussed.

## 2. Experimental procedures

The alloys investigated were melted in a vacuum induction furnace. They were homogenized at 1120°C for 24 h and forged into  $\phi 40$  mm rods, then rolled into  $\phi 20$  mm rods. The samples were solution treated at 1120°C for 24 h in vacuum, then aged at 980°C for 1 h, 775°C for 12 h and 620°C for 8 h. The cooling rate was 55°C per h. Table

\*Corresponding author. Tel.: +86-10-6245-8133; fax: +86-10-6245-6925.

E-mail address: rongming.wang@biam.ac.cn (R.M. Wang).

Table 1  
Chemical composition of the investigated superalloy (wt.%)

	Ni	Co	Nb	Ti	Al	Si	C	Y	La	Fe
Conventional	38.10	14.00	4.70	1.55	0.09	0.20	0.03	–	–	rest
Y-Containing	38.14	13.38	4.52	1.40	0.09	0.20	0.03	trace	–	rest
La-Containing	38.14	13.38	4.60	1.78	0.09	0.20	0.03	–	trace	rest

1 shows the chemical compositions of the alloys investigated.

Specimens for transmission electron microscopy (TEM) were done by twin jet electrolytic polishing. The electrolytic solution is 10 vol. % perchloric acid in ethanol under the condition of about 90 V at  $-20^{\circ}\text{C}$  or below. Conventional TEM analysis was performed on an H-800 and JEOL 2010 transmission electron microscopes operated at 200 kV. High-resolution (HR) images were obtained on JEOL 2000EX II microscope at 200 kV. Phases was extracted and separated using electroanalysis. The electrolytic solution to extract  $\gamma'$ , platelet, Laves and NbC phases was 5%  $\text{HNO}_4$ +2%  $\text{HClO}_4$ + $\text{CH}_3\text{OH}$  and that to extract platelet, Laves and NbC phases was 5%  $\text{HCl}$ +5% glycerin+2% tartaric acid+ $\text{CH}_3\text{OH}$ . The electrolytic currents are both  $0.1\text{A cm}^{-2}$  at  $-5^{\circ}\text{C}$ . The difference is the content of  $\gamma'$  phase. The Laves and NbC phases were separated from the platelet phase by putting the powders into 6% $\text{H}_2\text{SO}_4$  and 2% tartaric acid liquid for 3 h at  $100^{\circ}\text{C}$ . The oxidation resistance of the alloy was expressed using increased weight when exposed at high temperature for long time. The stress rupture strength of the alloy was expressed by rupture life at test conditions  $540^{\circ}\text{C}$  and 825 MPa.

### 3. Results and discussion

Investigations reveal that the oxidation resistance of the alloy improves significantly with appropriate rare earth element addition. Table 2 gives the effect of the rare earth on the oxidation resistance of the alloy at  $650^{\circ}\text{C}$ . The results indicate that the oxidation resistance can be improved after the alloy is exposed at high temperature for long time. The advantage becomes more distinct with extended time.

In the meantime, the stress rupture strength of the alloy improves a lot with trace Y addition. The rupture lives at

Table 2  
The effect of the rare earth on the oxidation resistance of the alloy at  $650^{\circ}\text{C}$

Rare earth element (trace)	Oxidation rate at $650^{\circ}\text{C}$ ( $\text{g m}^{-2}\cdot\text{h}$ )				
	100 h	300 h	500 h	700 h	1000 h
–	0.263	0.124	0.087	0.115	0.226
Y	0.192	0.130	0.072	0.072	0.051
La	0.202	0.112	0.070	0.067	0.072

testing conditions  $540^{\circ}\text{C}$  and 825 Mpa of the conventional alloy and the Y-containing alloy are measured to be about 50 and 200 h, respectively. However, the stress rupture strength of the alloy remains almost the same with trace La addition. Moreover, the mechanical properties, such as strength, and physical properties, such as coefficient of thermal expansion, remain almost identical with Y or La addition. It indicates that adding appropriate yttrium during fabrication is an effective way to improve the overall properties of the alloy.

It is commonly acknowledged that the change of microstructures lead to change in the properties. Fig. 1 shows the optical micrographs of the alloys investigated. It can be found that the grain size of the alloy is much smaller with appropriate yttrium addition. The grain size of the conventional alloy is about  $100\ \mu\text{m}$  in average and in the range of  $20\text{--}200\ \mu\text{m}$ . The average size of the yttrium-containing alloy is about  $60\ \mu\text{m}$  in the range of  $10\text{--}120\ \mu\text{m}$ . Fig. 2 shows the bright field images of the alloys investigated. The images of Fig. 1 and Fig. 2 indicate that a large amount of the platelet precipitates separates out in the yttrium-containing alloy and the precipitates are smaller and denser than those in the conventional alloy.

Analytical electron microscopy study reveals that the platelet phase in the yttrium-containing alloy is H phase, which has a  $\text{Cu}_5\text{Ca}$ -type crystal structure with lattice parameters  $a=0.498\ \text{nm}$  and  $c=0.408\ \text{nm}$  [9]. The space group is  $P6/mmm$  and the molecule satisfies  $(\text{Fe}, \text{Ni}, \text{Co})_5(\text{Nb}, \text{Ti}, \text{Si})$ . Previous work also indicated that that the platelet phase in the conventional alloy is  $\epsilon$  phase, which can be described as  $(\text{Fe}, \text{Ni}, \text{Co})_3(\text{Nb}, \text{Ti}, \text{Si})$  [4,5]. The relatively low content of Nb, Ti and Si in H phase compared with that in  $\epsilon$  phase leads to more platelet precipitates with appropriate yttrium addition, which is beneficial to the stress rupture strength of the alloy.

The results of chemical analysis confirm the conclusion above. Table 3 gives the content of the various precipitates that exist in the investigated alloys. The content of the platelet precipitates raises from 0.87% to 1.289% with trace yttrium addition. The content of Laves and NbC phases decreases from 0.30% to 0.224%, which indicates that trace rare earth element prevents the formation of laves phase and carbide in the alloys investigated. The content of  $\gamma'$  phase /remains almost the same with trace yttrium addition, which ensures the good properties of the conventional alloy, such as strength, coefficient of thermal expansion, etc.

In order to investigate the reason how the rare earth

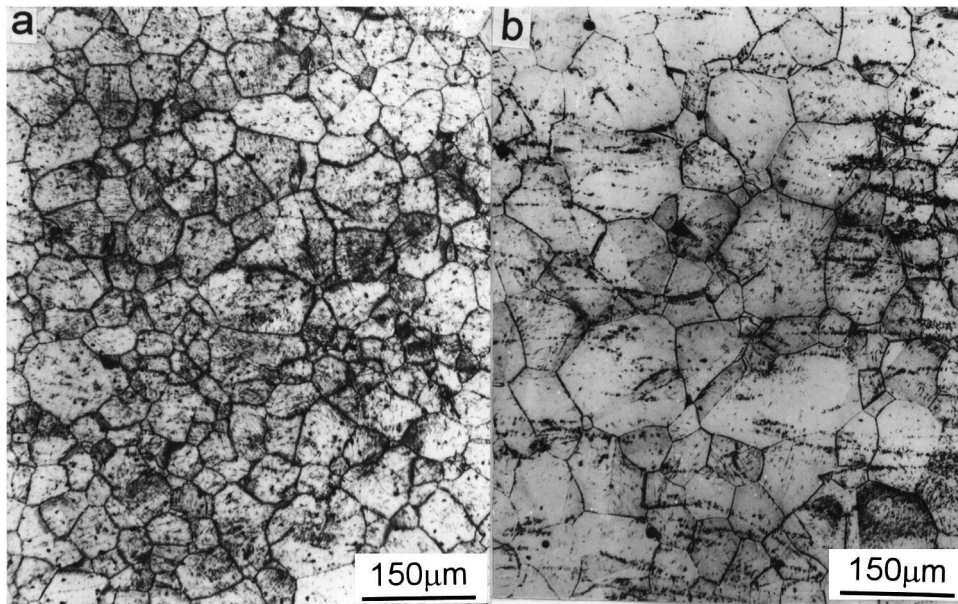


Fig. 1. Optical micrographs of the alloys investigated (a) conventional alloy, (b) yttrium-containing alloy.

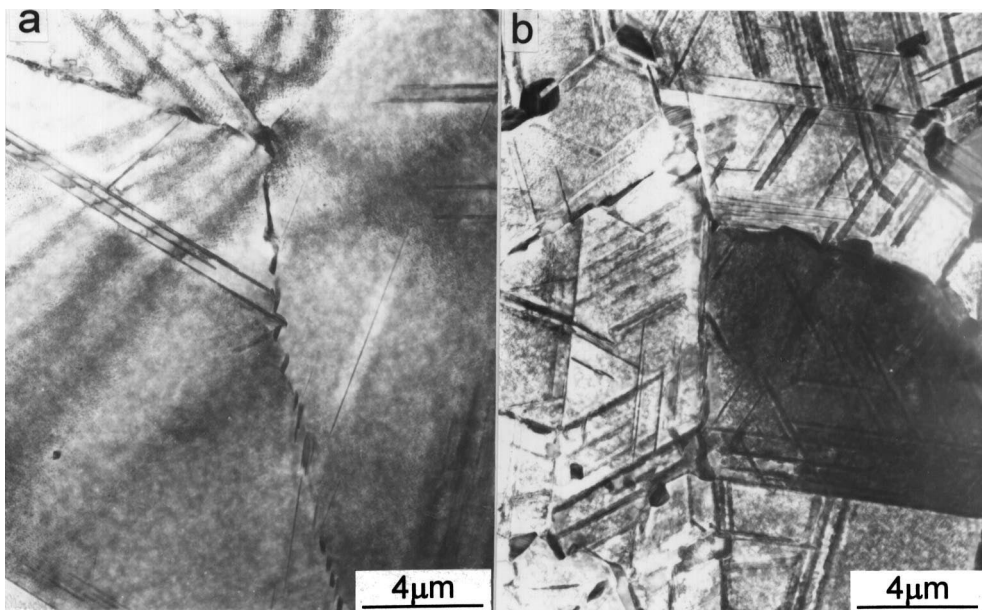


Fig. 2. Bright field images of the platelet precipitates in the alloys investigated (a) conventional alloy, (b) yttrium-containing alloy.

element affects the microstructure and results in the phase transformation, it is necessary to study the distribution of rare earth element in the alloy. However, it is hard to analyze it using energy dispersive X-ray spectroscopy since yttrium content is very low. One effective way to

analyze trace element is chemical analysis. Table 4 shows the distribution of yttrium in the precipitates in Y-containing alloy using chemical analysis. From Table 4, it can be found that yttrium segregates at H phase. The content of yttrium in  $\gamma'$ , Laves and carbide is very low. Then H phase

Table 3  
Content table of the precipitates in the investigated alloys (wt.%)

Alloy	$\gamma'$	Platelet phase	Laves +NbC
Conventional	15.2	0.87 ( $\epsilon + \epsilon'$ phase)	0.30
Y-containing	14.27	1.289 (H phase)	0.224

Table 4  
Distribution of yttrium in the precipitates in Y-containing alloy (wt.%)

Phases	$\gamma'$ +H+Laves+NbC	H+Laves+NbC	H	Laves+NbC
Content	0.00754	0.00731	0.00644	0.00029

can be described as  $(\text{Fe, Ni, Co})_5(\text{Nb, Ti, Si, Y})$ . It indicates that yttrium is the reason that causes phase transformation of the platelet precipitate in the alloy.

More research indicates that the H phase and the  $\gamma'$  phase exhibit a definite orientation relationship, which can be described using a typical one as  $(\bar{1}\bar{1}\bar{1})_{\gamma} // (0001)_{\text{H}}$ ,

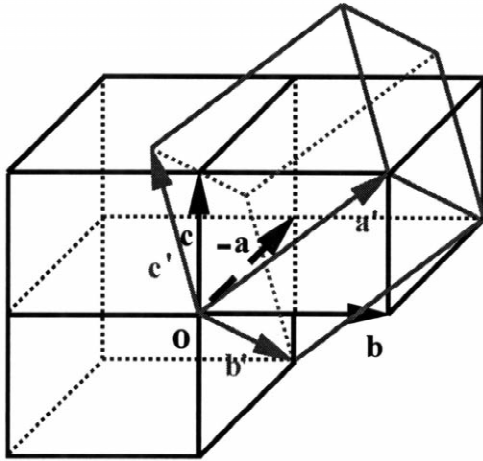


Fig. 3. Diagram of the crystallographic orientation relationship between the H phase and the matrix. Here  $a, b$  and  $c$  are unit vectors of the matrix;  $a', b'$  and  $c'$  are unit vectors of the H phase.

$[\bar{1}\bar{1}0]_{\gamma} // [1\bar{1}\bar{2}]_{\text{H}}$  [9]. It indicates that the closed planes and directions of the two phases are parallel to each other. Then the diagram of crystallographic orientation relationship between the H phase and the matrix can be obtained, as shown in Fig. 3, where  $a, b$  and  $c$  are unit vectors of the matrix while  $a', b'$  and  $c'$  are unit vectors of the H phase.

Fig. 4 gives a high-resolution image of the H phase and the matrix. The incident beams are parallel with  $[\bar{1}\bar{1}\bar{2}]_{\text{H}} // [011]_{\gamma}$  and the interfaces are parallel with  $(000\bar{1})_{\text{H}} // (\bar{1}\bar{1}\bar{1})_{\gamma}$ . The interface, as indicated by double arrows, is very clean, smooth and straight. The interplanar spacing of  $(000\bar{1})$  plane and  $(1\bar{1}00)$  plane in H phase are 0.408 nm and 0.432 nm, respectively. The atomic spacing of the H phase and the matrix in the interface are 0.432 nm and 0.221 nm, respectively, which gives a semicoherent interface where every two  $(\bar{1}\bar{1}\bar{1})_{\gamma}$  atoms correspond to one  $(000\bar{1})_{\text{H}}$  atom group with a mismatch of about one percent. The semicoherent interface between H phase and the matrix makes the lowest interface energy and relatively low aberration energy, which is beneficial to the stability of the alloy.

The grain boundary of the conventional alloy consists of  $\epsilon$ , Laves, O and T phases [10], as shown in Fig. 2(a). However, the grain boundary of the yttrium-containing alloy consists of H and O phases, as shown in Fig. 2(b). The precipitates of H phase along the grain boundary

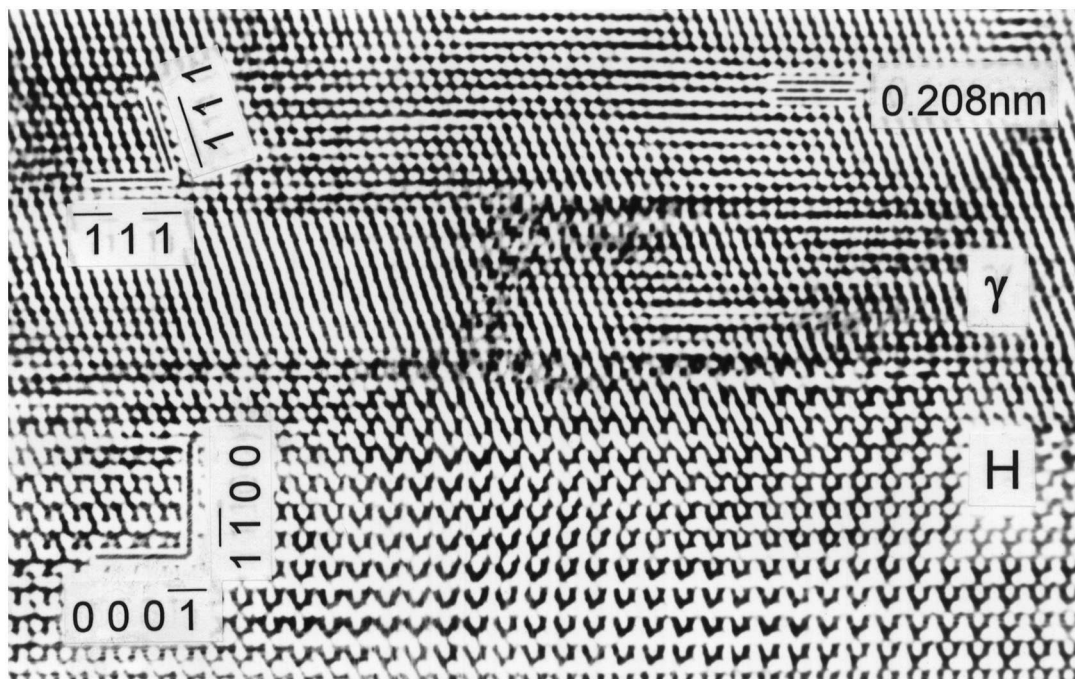


Fig. 4. High resolution images of the H phase and the matrix.

prevent oxygen from diffusing into the inner of the grain along the grain boundary, which improves the oxidation resistance of the alloy significantly.

#### 4. Conclusions

1. The oxidation resistance and stress rupture strength of the Fe–Ni–Co–Nb–Ti–Si superalloy improves significantly with trace additions of yttrium. The elevated temperature stability of the alloy also improves, which indicating selective addition of rare earth element during fabrication is an effective way to tailor the properties of the alloy.
2. The improvement in stress rupture life due to the addition of yttrium in the alloy results from the change of platelet precipitates. It transforms from  $\epsilon$  phase into H phase with more content and smaller and denser morphology.
3. The increase of oxidation resistance due to the addition of yttrium results from the change of grain boundary precipitates. In the yttrium-containing alloy, H phase forms along the grain boundaries as well as in the matrix and becomes the dominant grain boundary phase.
4. The yttrium segregates at the H phase and the molecule is written as  $(\text{Fe, Ni, Co})_5(\text{Nb, Ti, Si, Y})$ .

#### Acknowledgements

Thanks to the Chinese Science Foundation of Aeronautics for supporting this research.

#### References

- [1] D.F. Smith, E.F. Clastworthy, D.G. Tipton, W.L. Mankins, in: *Superalloys*, ASE, Metals Park, OH, 1980, pp. 521–530.
- [2] M.M. Morra, R.G. Ballinger, J.S. Hwang, *Metall. Trans. A* 23A (1992) 3177–3192.
- [3] K. Sato, T. Ohno, *J. Mater. Eng. Perform.* 2 (4) (1993) 511–516.
- [4] D.F. Smith, J.S. Smith, S. Floreen, in: *Proc. 5th Int. Symp. on Superalloys*, Seven Springs, PA, Superalloys, ASM, Metals Park, OH, 1984, pp. 591–600.
- [5] K.A. Heck, D.F. Smith, D.A. Wells, M.A. Holderby, in: S. Reichman, D.N. Duhl, G. Maurer, S. Antolovich, C. Lund (Eds.), *The Metallurgical Society, Superalloys*, 1988, pp. 151–160.
- [6] N. Duhl, G. Maurer, S. Antolovich, C. Lund, in: *Proc. Conf. The Metall. Soc.*, 1988, pp. 151–160.
- [7] W. Lu, *Acta Metall Sinica* 29 (1993) A307.
- [8] D.B. Zhang, C.J. Wu, *Acta Metall Sinica* 24 (1988) A100.
- [9] G.C. Zhao, W.S. Song, in: *Rare Earth Applications in Steels*, Metallurgical Press, 1987, p. 282.
- [10] R.M. Wang, C.Z. Li, D.H. Ping, M.G. Yan, *Mater. Sci. Eng. A* 241 (1998) 83.